Chemical Engineering Journal 161 (2010) 397–402

Contents lists available at ScienceDirect

Chemical Engineering Journal

journal homepage: www.elsevier.com/locate/cej

Hierarchical pore ZSM-5 zeolite structures: From micro- to macro-engineering of structured catalysts

B. Louis[a,*], F. Ocampo[a], H.S. Yun[b,*], J.P. Tessonnier[c], M. Maciel Pereira[d]

[a] Laboratoire des Matériaux, Surfaces et Procédés pour la Catalyse (LMSPC), UMR 7515 du CNRS, Part of European Laboratory for Catalysis and Surface Science (ELCASS), University of Strasbourg, 25 rue Becquerel, 67087 Strasbourg Cedex 2, France
[b] Center for Future Technology, Korea Institute of Materials Science, 531 Changwondero, Changwon, Republic of Korea
[c] Fritz-Haber-Institut der Max-Planck-Gesellschaft, Faradayweg 4-6, D-14195 Berlin, Germany
[d] Instituto de Quimica, Universidade Federal do Rio de Janeiro, Rio de Janeiro, RJ, Brazil

ARTICLE INFO

Article history:
Received 28 April 2009
Received in revised form 8 July 2009
Accepted 23 September 2009

Keywords:
ZSM-5 zeolite
Structured catalyst
Hierarchical porosity
n-Hexane cracking
Mesoporous zeolite

ABSTRACT

Zeolite crystals coated on mesoporous glass materials with hierarchical tri-modal pore size distributions have been successfully prepared and characterized. Starting glass monoliths, having regular meso- and macro-pores, were partly re-constructed into zeolite material, thus introducing additional microporosity via the growth of these zeolite crystals.

Hierarchical 3D porous glass scaffolds were prepared by a combination of sol–gel, double polymer templating, and rapid prototyping (RP) techniques. Structured zeolitic catalytic materials were produced by conventional self-assembly of template cations and silica species on the glass surface. Zeolite crystals are therefore in an intimate contact with the glass support, featuring micropores in addition to the mesopores.

A higher catalytic performance and selectivity toward low alkenes were achieved in *n*-hexane cracking reaction over these zeolite/glass composites in comparison with purely microporous zeolite materials.

1. Introduction

Zeolites represent an important class of materials with numerous technical applications in chemical industry, as ion-exchangers, sorbents or heterogeneous catalysts [1–4]. However, their uses in catalysis remain restricted to petrochemical processes owing to the shape-selectivity provided by their well-defined microporous structure and strong acidity. Zeolites offer great possibilities to conduct highly selective catalytic transformations as they exhibit an impressive number of different structures.

Zeolite catalysts are usually placed in catalytic fixed beds, as randomly packed powdered microgranules or extrudated pellets of millimeter size. The use of dumped packed beds leads to major drawbacks: mass transfer limitations, high pressure drop along the catalytic bed, rapid deactivation by coking, non-regular flow pattern, which can lead to reduced selectivity towards targeted products.

Since two decades, many studies were performed to develop structured zeolitic beds, via binderless coatings of zeolite crystals on metals or ceramics, to overcome these disadvantages [5–18]. Recently, several groups tempted to enhance the mass transfer in zeolite-catalyzed reactions, either via reducing the size of the crystals (down to few nanometers) to shorten the diffusion paths [7,19–21], or by raising the zeolite pore size [22,23].

Another approach to solve the diffusion problems consisted of introducing mesoporosity within the microporous crystal, leading to the hierarchization of zeolite pore structure [24–26]. Louis et al. made an attempt to allow the crystallization of zeolites on porous glass supports under strong alkaline conditions [10]. The glass matrix was partially transformed into zeolite crystals giving birth to a composite material with a micro/macro-bimodal pore system.

Following this strategy, the aim of the present work is to prepare new binderless and structured ZSM-5 zeolite coatings via an in situ hydrothermal synthesis on perfectly defined glass scaffolds. The latter already contain giant-, macro- and meso-pores, forming a monolith with hierarchical porosity. The knowledge and technology set up by Yun et al. enabled a perfect tailoring of pore sizes and structures, being thus controlled in a well-interconnected 3D porous system [27,28].

We aim therefore to combine an engineering of the zeolite catalyst at a triple-scale level of porosity: micro- and meso- together with appropriate macro-porosity. Our objective is to prepare new structured catalytic beds made of 3D tri-modal glass supports which exhibit improved hydrodynamics (compared to traditional

* Corresponding author.
E-mail addresses: blouis@chimie.u-strasbg.fr (B. Louis), yuni@kims.re.kr (H.S. Yun).

1385-8947/$ – see front matter © 2009 Elsevier B.V. All rights reserved.
doi:10.1016/j.cej.2009.09.041

packed beds), and that will combine both interesting advantages of structured zeolitic catalysts and tailored porosity. These catalysts activity and selectivity were evaluated in the *n*-hexane cracking reaction.

2. Experimental

2.1. Synthesis of the mesoporous glass scaffolds

Gel pastes for robotic deposition were prepared using tetraethyl orthosilicate (TEOS) as inorganic precursors, a triblock copolymer (Pluronic P123, $EO_{20}PO_{70}EO_{20}$, M_{ave} = 5750), as the meso-structure-directing agent through an evaporation-induced self-assembly process, and methyl cellulose (MC, M_{ave} = 86000), acting both as semi-macro-structure directing agent and binder [27,28]. First, the triblock copolymer was dissolved in ethanol. After, TEOS was mixed with a hydrochloric acid solution (1 M) under vigorous stirring, before ethanol and distilled water addition. The solution was sealed and aged at 40 °C for 24 h without stirring, and evaporated at 40 °C for 10–24 h without the seal until the volume of reactant solution reduced to one-fifth [27,28]. Finally, 1.4 g of methylcellulose (MC) template was mixed with this solution, leaving a homogeneous gel paste.

3D scaffolds were fabricated by directly excluding the paste gel onto a heated substrate using a robotic deposition device. A commercially available gantry robotic deposition apparatus was used with specially altered systems such as an actuator and heat-control to control the position of deposition nozzle for scaffold fabrication. The gel paste housed in the syringe was deposited through a cylindrical nozzle (17–26 gauge (G), 24 G (≈500 μm) is generally used). A linear actuator served to depress the plunger of the syringe at a fixed speed such that the volumetric flow rate could be precisely controlled. The excluding strength and speed is controlled 200–250 μL/min and 5–10 mm/s, respectively, depending on the viscosity of the gel paste. The gel paste excluded onto heated substrate (60–100 °C) to the fast condensation followed by both the solvent evaporation and the solidification of MC. The shapes and sizes of scaffold can be tailored at will and can be controlled by computer system. The fabricated organic–inorganic hybrid scaffolds were aged at 40 °C for 24 h and treated at 500–700 °C to remove the organic polymer template for obtaining the final calcined porous scaffolds.

2.2. Preparation of the zeolite coatings on porous glass scaffold

The synthesis mixture was prepared by adding at room temperature sodium aluminate, sodium chloride, tetrapropylammonium hydroxide in distilled water. Afterwards, the silica source (TEOS or aerosil 200) was introduced under vigorous stirring. The mole ratio was as follows: TPA-OH:Si:NaCl:$NaAlO_2$:H_2O = 2.16:5.62:3.43:0.13:1000. Once the gel has formed, ageing and homogenisation of the mixture were performed during 2 h. Then, the stirring was stopped and mesoporous glass monoliths (35 mg per piece) were placed into the synthesis mixture for 30 min. The gel was then poured in a 75 mL Teflon-lined autoclave containing the support packing. The temperature was increased within 1 h up to 443 K. The synthesis time was varied between 17 and 48 h. The packing was recovered upon filtration, washed with distilled water and dried at 373 K for 2 h. Then, the composite was kept in an ultrasonic bath (45 kHz) for 20 min to remove loosely attached crystals and dried at 373 K for 2 h. Finally, the monolith was calcined at 753 K in air for overnight to remove the template. The zeolite coated on the monolith was in its sodium form, and thus was exchanged three-times with ammonium chloride (0.1 M) at 348 K and finally calcined at 753 K for 5 h in air to get the zeolite in its H-form.

2.3. Characterizations

Specific surface areas (SSA) of the different materials were determined by N_2 adsorption–desorption measurements at 77 K by employing the BET method (Micrometrics sorptometer Tri Star 3000). Prior to N_2 adsorption, the sample was outgassed at 523 K overnight to desorb moisture adsorbed on the surface and inside the porous network.

X-ray diffraction patterns (XRD) were recorded on a Bruker D8 Advance diffractometer with a VANTEC detector side and Ni filtered Cu Kα radiation (1.5406 Å) over a 2θ range of 0.5–60° and a position sensitive detector using a step size of 0.02° and a step time of 2 s. The degree of crystallinity (Q) was calculated on the basis of the ratio between the sum of the seven higher reflections, referred to this ratio of the most crystalline sample, set arbitrary to unity [29].

SEM images were acquired with a Hitachi S4800 FEG microscope equipped with an EDS system (EDAX) for elemental analysis. The samples were loosely dispersed on a conductive carbon tape to preserve the as-prepared morphology as much as possible. SE images were acquired at low accelerating voltage, *i.e.* 1.5 kV, for better sensitivity to surface features. EDX spectra were acquired at an accelerating voltage of 15 kV.

The microstructure of the samples was investigated by transmission electron microscopy (TEM). The investigation was conducted in a Philips CM200 microscope with a LaB_6 emitter. The samples were dispersed in chloroform and deposited on a holey carbon film supported on a Cu grid. The measured lattice spacings were compared with the reference X-ray powder diffraction pattern of the International Centre for Diffraction Data (ICCD 84039 file).

The Brönsted acidity of the materials was evaluated by means of an H/D isotope-exchange technique, developed in our group [30–32], which counts the total number of O–H groups (with no information about their acid strength). This technique also allows a precise determination of the chemical composition of as-synthesized zeolite, and hence a valid estimation of the mass of zeolite coated in the final composite material [32].

The *n*-hexane cracking has been chosen as a model reaction. The reactions were either carried out at 773 K or 873 K, during 2 h under nitrogen, using 0.03 g of catalyst. The paraffin was kept at room temperature in a saturator and then directed to the reactor using pure nitrogen as carrier gas. The reaction products were analyzed on-line by gas chromatography (Shimadzu GC-2010, Chrompack KCl/Al_2O_3 column, FID detector) after different times on stream.

3. Results and discussion

3.1. Characterization of the zeolite/glass composites

Hierarchical 3D porous glass monoliths were prepared by a combination of the sol–gel, double polymer templating, and rapid prototyping (RP) techniques as shown in Fig. 1. The glass monolith exhibits three pore families: giant-sized pores (300–500 μm) produced by the RP technique (Fig. 1a), macro-sized pores (10–100 μm) made using a methyl cellulose template (Fig. 1b), and meso-sized pores (4–5 nm) with 2D hexagonal pore structure produced by P123 triblock copolymer self-assembly (Fig. 1c). These starting hierarchized porous glass monoliths lack in microporosity, before the zeolite coating process.

ZSM-5 crystals were grown on mesoporous glass while using TEOS or aerosil 200 as silica source and varying the synthesis time between 17 and 48 h. After each experiment, both the recovered

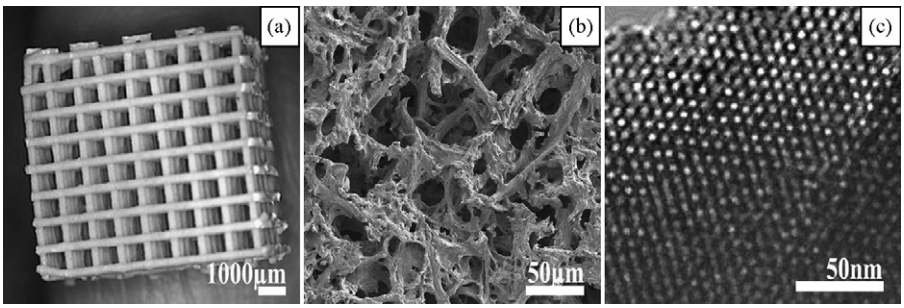

Fig. 1. Optical (a), FE-SEM (b), and TEM (c) images of hierarchically giantporous (a), macroporous (b), and mesoporous (c) glass monolith.

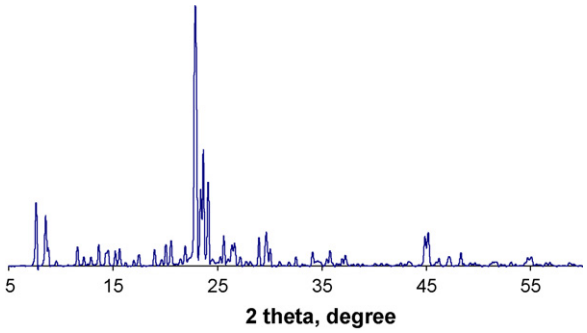

Fig. 2. XRD pattern of ZSM-5 crystals on mesoporous glass (aerosil 200 as Si-source) after 17 h of synthesis.

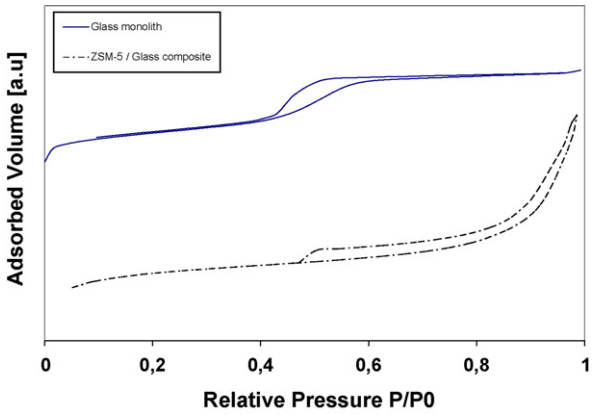

Fig. 3. Nitrogen adsorption–desorption isotherms for bare monolith and ZSM-5/glass composite.

monolith piece and the unsupported powder (settled at the bottom of the autoclave) were weighted. A zeolite synthesis performed during 48 h led to the complete dissolution of the monolith due to the strong alkalinity of the medium (pH = 14). Hence, only powder with few pieces of starting glass substrate can be recovered. The advantages expected owing to the creation of a hierarchical material were completely lost. In order to prevent this phenomenon, the synthesis time was decreased to 24 h, resulting in the recovery of about 30% from starting monolith. Again, the synthesis time was decreased to 17 h and 88% from the initial monolith could be recovered. According to these results, one could state that reducing the synthesis time limits the dissolution of the glass substrate, thus protects the structured macro-shaped monolith. However, the synthesis time cannot be further shortened, as it would result in the formation of only partially crystalline zeolitic material. One should therefore find a compromise between the amount of zeolite crystals coated on the surface to prevent it from dissolution, but not too many in order to keep a thin layer of catalyst (active phase), that insures the advantages of structured materials.

The crystallinity of the different alumino-silicate coatings was investigated by means of XRD technique. Fig. 2 presents the diffraction pattern of the ZSM-5 prepared with aerosil 200 after 17 h. Furthermore, all as-prepared materials using TEOS at different synthesis duration, exhibit a high crystallinity (Figure not shown) characteristic of the MFI structure [33]. Obviously, the powdered samples showed a higher crystallinity (set arbitrary as reference to 1) than the composite monoliths constituted by a zeolite layer coated on a glass support. In the latter, part of the composite is constituted by inert glass. However, both monoliths recovered after 17 and 24 h remained highly crystalline (0.77), thus confirming the coating of MFI crystals on the support. Moreover, while using aerosil 200, a successful coating of ZSM-5 crystals on the support exhibited high crystallinity (0.74) was also possible after 17 h of synthesis (Fig. 2).

Detailed characteristics of zeolite/glass scaffold composites were studied by BET and are presented in Table 1. The SSA values reached respectively 453 m^2/g for the ZSM-5/glass composite using TEOS after 17 h of synthesis, and 409 m^2/g when using aerosil 200. Since powdered MFI-type zeolite prepared with the same gel composition exhibits a SSA of 320 m^2/g and the starting mesoporous glass support possesses a SSA of 520 m^2/g, the quantity of zeolite coated was roughly estimated to 33.5 wt% for the former, and to 44.5 wt% for the latter. In a previous study, we have shown that the use of aerosil 200, rather than TEOS, led to a higher amount of zeolite produced [34]. The mesoporous character of zeolite/glass monolith composite was further observed both by the porous volume values for the composites, between 0.17 and 0.18 cm^3/g and remaining S_{meso} = 28% (Table 1). Furthermore, it appears from nitrogen adsorption–desorption isotherm (Fig. 3), that the presence of a hysteresis loop at relative pressures higher than $P/P_0 > 0.4$, indicates the persistence of mesopores after the zeolite synthesis.

Hence, initial hierarchized giant-, macro-, meso-porosities are complemented by microporosity due to the zeolite material.

Table 1
Characteristics of ZSM-5 zeolite coatings on mesoporous glass depending on the Si-source present in the gel.

	SSA [m^2/g]	Porous volume [cm^3/g]	Amount of zeolite coating [%]
Monolith	520	0.246	0
ZSM-5 powder	320	0.117	100
Composite/TEOS	453	0.169	33.5
Composite/aerosil 200	409	0.177	44.5

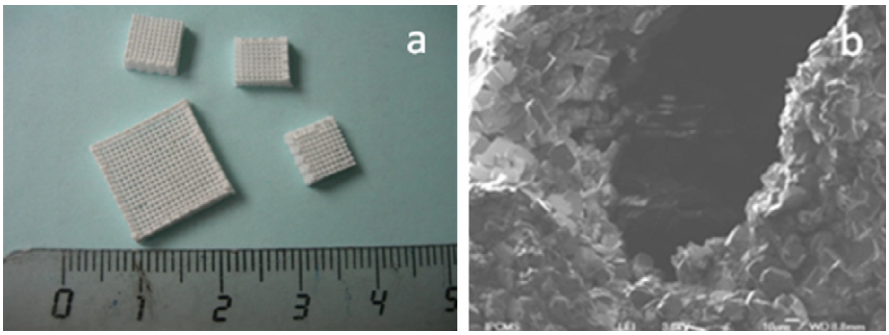

Fig. 4. (a) Mesoporous glass monoliths and (b) SEM image of ZSM-5 crystals coated on a monolith.

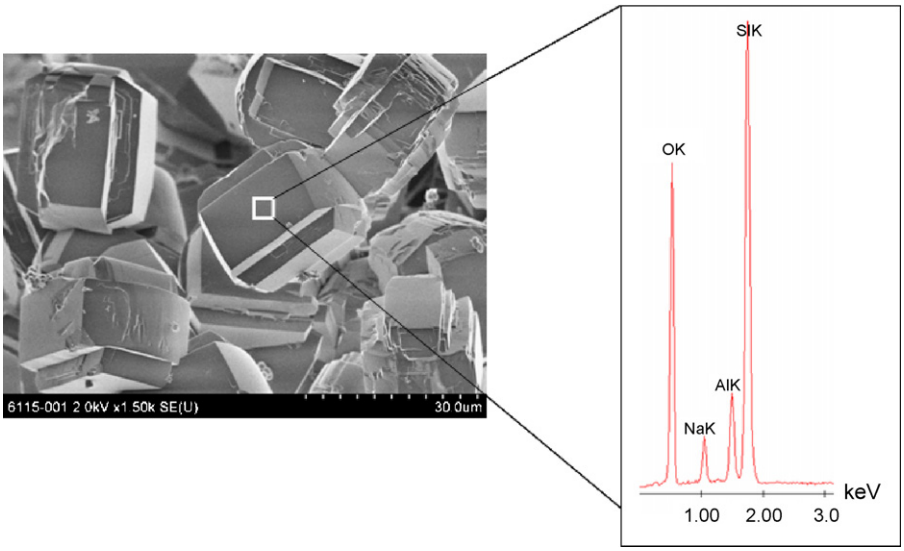

Fig. 5. SEM-EDX of Na-ZSM-5 zeolite crystal.

SEM micrographs of glass monoliths recovered after a synthesis time of 17 h using TEOS (Fig. 4a and b) as Si-source confirmed the characteristic prismatic crystals (having 20 μm in length) of the MFI structure, which homogeneously cover the surface of the glass support. Interestingly, the so-called giant-pores remain preserved, and homogeneously covered by zeolite material (Fig. 4b). At higher magnification of the zeolite (Fig. 5a), the elemental composition of a zeolite crystal was obtained by EDX analysis (Fig. 5b); the Si/Al ratio was estimated to 20 ± 2.

The microstructure of the zeolite/glass composite was investigated by transmission electron microscopy (TEM). Fig. 6 presents TEM image of ZSM-5 coated on a glass monolith (using TEOS, 17 h of synthesis) and shows the edge of a zeolite crystal. The periodic lattice fringes confirm that the zeolite is well crystallized. Square-shaped holes of 10–20 nm in diameter, randomly distributed in the structure, were also clearly observed.

From these characterizations, it appears that initial mesoporosity present in the structured glass monolith (Fig. 1c) was partially destroyed during the zeolite synthesis. However, part of this mesostructure was maintained, thus confirming the presence of micro-, meso-, and macro-porosity. The calculated fast Fourier transform (FFT) of the image (inset of Fig. 6) gives a lattice spacing of 9.99 Å, which corresponds to the (2 0 0) plane of the ZSM-5 (theoretical value is 9.94 Å) [33]. However, in order to exclude the sole presence of MFI domains having different orientations, or MFI and MEL phases intergrowth, hence to further support the presence of mesoporosity, low-angle diffraction pattern is shown in Fig. 7. The

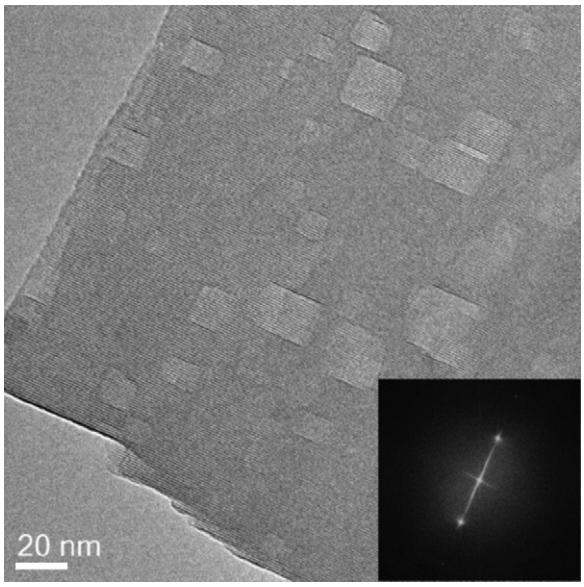

Fig. 6. TEM image of the edge of a MFI zeolite crystal. Inset: FFT of the image.

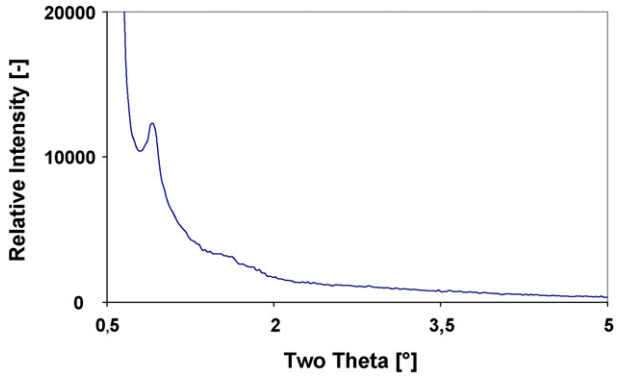

Fig. 7. Low-angle powder diffraction pattern of zeolite–glass composite.

diffraction at $2\theta = 0.9^{\circ}$, undoubtedly proves the presence of mesopores having approximately 16 nm in size (based on hexagonal unit cell calculations), as expected from TEM images.

3.2. Estimation of mass transfer limitations

In heterogeneous-catalyzed reactions by zeolites, mass transfer limitations have to be taken into account, especially to prove any improvement brought by the zeolite mesoporosity. The estimation of Thiele-Weisz modulus has therefore been undertaken according to the following formula: $\Phi = L(k_V/D_{eff})^{(1/2)}$, where L represents the diffusion length, k_V the rate coefficient, and D_{eff} corresponds to the effective diffusivity of *n*-hexane in the zeolite pores. A Thiele-Weisz moduli for mesoporous zeolite coated on glass monolith $\Phi \sim 0.01$ was calculated, whereas $\Phi \sim 4$ was estimated for ZSM-5 microcrystals (Fig. 6). In terms of intra-particle transport, such low values for Weisz modulus (admitted when $\Phi < 0.1$) confirms a full utilization of zeolite catalyst particle, thus the reaction rate equals the intrinsic reaction rate. The composite materials operate efficiently and exclude mass transfer limitations. Whereas, the performance of ZSM-5 microcrystals is seriously affected by diffusion constraints, since only part of the catalyst is used for the reaction.

3.3. Zeolite/glass catalysts: evaluation of their efficiency in n-hexane cracking

The acidity and the catalytic activity of the composite HZSM-5/glass were investigated in the *n*-hexane cracking reaction and the results were compared to a powdered commercial HZSM-5 (Si/Al = 12, Petrobras, Brazil). According to BET results (Table 1), the amount of zeolite material coated was roughly estimated to 33.5 wt% on the glass when using TEOS as Si-source. The quantity of zeolite crystals grown on the monolith was further confirmed by H/D exchange acidity measurements, and was assessed to 26 wt% on the glass support. Our isotope-exchange technique is a powerful indirect tool to estimate the amount of zeolite coated on several supports [32]. Another advantage of the structured catalytic system is the open structure given by the glass monolith which leads to a moderate pressure drop along the catalyst bed as compared to that observed on the extrudated pellets or powdered catalysts [35]. We have recently shown that the pressure drop reached was equal when the gas velocity is one and a half higher through the 3D monolithic structured bed when compared to extrudates [36]. One can therefore argue that ZSM-5/glass structured composites exhibit an improved hydrodynamics, in terms of pressure drop and mass transfer for its use in gas phase reactions.

Preliminary experiments of *n*-hexane cracking were performed (Table 2) to see whether these structured zeolites having hierarchical porosity exhibit both the strong Brönsted acidity required for this reaction and the advantages gained from their pore engineering. It is noteworthy that the higher rate of *n*-hexane consumption is in favour of mesoporous ZSM-5 zeolite coated on glass monolith, *i.e.* 3.54 against 0.54 for the commercial zeolite that contains even more Brönsted acid sites (rates are expressed in [mol/g min]). Since the leading work from Haag and Dessau, where a linear dependence between the number of Brönsted acid sites and *n*-hexane cracking activity was reported [37], it appears that our structured zeolite is more active than the commercial catalyst (Si/Al = 12), even with a lower number of Brönsted acid sites (Si/Al = 20). These results are in line with previous studies reporting a higher activity of mesoporous zeolites in acid-catalyzed transformations [26,38–40].

Moreover, HZSM-5/glass exhibits an improved selectivity toward light olefins (alkene-to-alkane ratio = 1.14 mol at 773 K), compared to the commercial catalyst (0.95). This particular selectivity is of potential interest since C_2–C_4 light olefins are important building blocks for the chemical industry, as monomers, or as starting compounds for the synthesis of fine chemicals. Higher propylene to ethylene ratio could also be achieved over the structured zeolite material, *i.e.* 5.8 whilst 2.5 was obtained with powdered commercial ZSM-5 zeolite. This higher selectivity toward alkenes can be explained by improved diffusion properties within the hierarchical zeolite crystals [40]. Alkenes, being more reactive than alkanes, are more easily transformed via acid-catalyzed pathways when mass transfers are hindered. While increasing the contact time between the products and the Brönsted acid sites, as it is the case of powdered zeolite, the alkene-to-alkane ratio will necessarily decrease.

Table 2 also presents the selectivities in ethylene and propylene respectively for different composite materials. A MFI zeolite grown on glass composite, where H-ZSM-5 crystals were prepared under acidic conditions [34]; and the results obtained with microporous ZSM-5 zeolite (prepared via the same alkaline gel) coated on a carbon support are presented for comparison. It appears that both ZSM-5 mesoporous zeolites coated on glass exhibited a higher reactivity in the *n*-hexane cracking reaction, *i.e.* 3.54 and 1.47 mol of alkane converted per gram of catalyst and per minute, for alkaline prepared and fluoride prepared composites, respectively. Microporous zeolite crystals coated on carbon support are one order of magnitude less active (0.24 mol of *n*-hexane converted per gram and per minute). In addition, the selectivity to propylene achieved over the mesoporous HZSM-5 (TEOS) zeolite over glass monolith remains also much higher, *i.e.* 0.35 against 0.25–0.26 for other zeolites which is in line with an improved diffusion of primary cracking products within the hierarchized zeolite porous network.

To summarize, our structured zeolite catalyst enables a high activity in *n*-hexane cracking (chosen as a model acid-catalyzed reaction), together with a higher selectivity toward valuable C_2–C_3 light olefins, when compared to commercial catalyst, which market demand is drastically increasing. These mesoporous glass supports

Table 2
Selectivity to ethylene and propylene and rate of *n*-hexane cracking at 873 K for the different zeolite catalysts.

Catalyst	Selectivity in ethylene	Selectivity in propylene	Rate of *n*-hexane cracking [mol/g min]
Composite/TEOS (Alkaline route)	0.13	0.35	3.54
Composite/TEOS (Fluoride route)	0.20	0.26	1.47
ZSM-5/carbon	0.15	0.25	0.24
ZSM-5 commercial	0.14	0.26	0.54

can therefore be a useful tool to promote zeolitization [41,42], to produce micro/mesoporous materials which can retain their structured macroscopic shape. Further catalytic studies are under progress to investigate the potentiality of these structured zeolite materials coated on glass monoliths.

4. Conclusion

ZSM-5 zeolite crystals were successfully grown on hierarchized meso-, macro- and giant-porous glass scaffolds. In addition to the microporosity gained from the zeolite, our approach led to introduce mesopores into the zeolite crystals. Further improvements should lead to the preparation of mesoporous zeolite crystals with highly ordered structures and with uniform pore sizes.

These structured zeolite catalysts exhibit strong acidic properties and were more active than commercial H-ZSM-5 catalyst in *n*-hexane cracking reaction. The composite material also enabled a higher selectivity toward light olefins, which are of primary interest in refining processes.

Since zeolite/glass composites are already in a monolithic form, it renders easier their application in practical processes. Following the same strategy, new zeolite materials with porosities of different length scales can be developed, thus leading to interesting hierarchical structures. These materials with multiple levels of intricacies and design parameters offer the possibility to engineer, at the same time, molecular, microscopic and macroscopic characteristics.

Acknowledgements

This work was supported by the Korea Science and Engineering Foundation (KOSEF) grant funded by the Korea government (MEST) (No. R01-2008-000-20037-0). The authors are grateful to Thierry Romero and Jean-Daniel Sauer for their technical assistance.

References

[1] A. Corma, Inorganic solid acids and their use in acid-catalysed hydrocarbon reactions, Chem. Rev. 95 (1995) 559–614.
[2] A. Corma, H. Garcia, Organic reactions catalysed over solid acids, Catal. Today 38 (1997) 257–308.
[3] A. Dyer, An Introduction to Zeolite Molecular Sieves, John Wiley & Sons Ltd., 1988.
[4] H. Ghobarkar, O. Schäf, U. Guth, Zeolites-from kitchen to space, Prog. Solid State Chem. 27 (1999) 29–73.
[5] J.M. Antia, R. Govind, Applications of binderless zeolite-coated monolithic reactors, Appl. Catal. 131 (1995) 107–120.
[6] H. van Bekkum, E.R. Geus, H.W. Kouwenhoven, Supported zeolite systems and applications, Stud. Surf. Sci. Catal. 85 (1994) 509–542.
[7] F.C. Buciuman, B. Kraushaar-Czarnetzki, Preparation and characterization of ceramic foam supported nanocrystalline zeolite catalysts, Catal. Today 69 (2001) 337–342.
[8] The present and the future of structured catalysts—An overview, in: A. Cybulski, J.A. Moulijn (Eds.), Structured Catalysts and Reactors, Marcel Dekker Inc., New York, 1998, p. 670.
[9] B. Louis, P. Reuse, L. Kiwi-Minsker, A. Renken, Synthesis of ZSM-5 coatings on stainless steel grids and their catalytic activity for partial oxidation of benzene by N_2O, Appl. Catal. A 210 (2001) 103–109.
[10] B. Louis, C. Tezel, L. Kiwi-Minsker, A. Renken, Synthesis of structured filamentous zeolite materials via ZSM-5 coatings of glass fibrous supports, Catal. Today 69 (1–4) (2001) 365–370.
[11] S. Mintova, V. Valtchev, L. Konstantinov, Adhesivity of molecular sieve films on metal substrates, Zeolites 17 (1996) 462–465.
[12] V. Valtchev, S. Mintova, The effect of the metal substrate composition on the crystallization of zeolite coatings, Zeolites 15 (1995) 171–175.
[13] V. Valtchev, S. Mintova, B. Schoeman, L. Spasov, L. Konstantinov, Zeolite crystallization on mullite fibers, Zeolites 15 (1995) 527–532.
[14] Y. Yan, T. Bein, Zeolite thin films with tunable molecular-sieve function, J. Am. Chem. Soc. 117 (1995) 9990–9994.
[15] Y. Yan, M.E. Davis, G.R. Gavalas, Preparation of zeolite ZSM-5 membranes by in-situ crystallization on porous alpha-Al_2O_3, Ind. Eng. Chem. Res. 34 (1995) 1652–1661.
[16] A. Zampieri, P. Colombo, G.T.P. Mabande, T. Selvam, W. Schwieger, F. Scheffler, Adv. Mater. 16 (2004) 819.
[17] A. Zampieri, S. Kullmann, T. Selvam, J. Bauer, W. Schwieger, H. Sieber, T. Fey, P. Greil, Micropor. Mesopor. Mater. 90 (2006) 162–174.
[18] S. Golapakrishnan, A. Zampieri, W. Schwieger, Mesoporous ZSM-5 zeolites via alkali treatment for the direct hydroxylation of benzene to phenol with N_2O, J. Catal. 260 (2008) 193–197.
[19] S. Mintova, N.H. Olson, V. Valtchev, T. Bein, Mechanism of zeolite. A nanocrystal growth from colloids at room temperature, Science 283 (1999) 958–960.
[20] A. Zabala Ruiz, H. Li, G. Calzaferri, Angew. Chem. Int. Ed. 45 (2006) 5282.
[21] F. Schüth, W. Schmidt, Adv. Mater. 14 (2002) 629–638.
[22] D.M. Poojary, J.O. Perez, A. Clearfield, J. Phys. Chem. 96 (1992) 7709–7714.
[23] K.G. Strohmaier, D.E.W. Vaughan, J. Am. Chem. Soc. 125 (2003) 16035–16039.
[24] K. Egeblad, C.H. Christensen, M. Kustova, C.H. Christensen, Chem. Mater. 20 (2008) 946–960.
[25] (a) M. Hartman, Angew. Chem. Int. Ed. 43 (2004) 5880;
(b) Y. Fang, H. Hu, G. Chen, Chem. Mater. 20 (2008) 1670–1672.
[26] (a) R. Garcia, I. Diaz, C. Marquez-Alvarez, J. Perez-Pariente, Chem. Mater. 18 (2006) 2283–2292;
(b) J. Perez-Pariente, C.H. Christensen, K. Egeblad, Christensen, H. Christina, J.C. Groen, Chem. Soc. Rev. 37 (2008) 2530–2542.
[27] H.S. Yun, S.E. Kim, Y.T. Hyeon, Chem. Commun. (2007) 2139–2141.
[28] H.S. Yun, S.E. Kim, Y.T. Hyun, S.J. Heo, J.W. Shin, Chem. Mater. 19 (2007) 6363–6366.
[29] S.A. Axon, J. Klinowski, Appl. Catal. 56 (1989) 9.
[30] B. Louis, S. Walspurger, J. Sommer, Catal. Lett. 93 (2004) 81–84.
[31] J.P. Tessonnier, B. Louis, S. Walspurger, J. Sommer, M.J. Ledoux, C. Pham-Huu, J. Phys. Chem. B 110 (2006) 10390–10395.
[32] S. Walspurger, B. Louis, Appl. Catal. A 336 (2008) 109–115.
[33] W.M. Meier, D.H. Olson, Atlas of Zeolite Structure Types, 3rd ed., Butterworth, London, 1992.
[34] J. Arichi, B. Louis, Cryst. Growth Des. 8 (2008) 3999–4005.
[35] S. Ivanova, B. Louis, B. Madani, J.P. Tessonnier, M.J. Ledoux, C. Pham-Huu, J. Phys. Chem. C 111 (2007) 4368–4373.
[36] S. Ivanova, E. Vanhaecke, B. Louis, S. Libs, M.J. Ledoux, S. Rigolet, C. Marichal, Ch. Pham, F. Luck, C. Pham-Huu, Chem. Sus. Chem. 1 (2008) 851–857.
[37] W.O. Haag, R.M. Lago, P.B. Weisz, The active site of acidic aluminosilicate catalysts, Nature 309 (1984) 589–591.
[38] Y. Sun, R. Prins, Appl. Catal. A 336 (2008) 11–16.
[39] C. Mei, Z. Liu, P. Wan, Z. Xie, W. Hua, Z. Guo, J. Mater. Chem. 18 (2008) 3496–3500.
[40] (a) I. Schmidt, A. Krogh, K. Wienberg, A. Carlsson, M. Brorsen, C.J.H. Jacobsen, Chem. Commun. (2000) 2157–2158;
(b) C.H. Christensen, K. Johannsen, E. Tornqvist, I. Schmidt, H. Topsoe, C.H. Christensen, Catal. Today 128 (2007) 117–122.
[41] V. Valtchev, M. Smaihi, A.C. Faust, L. Vidal, Angew. Chem. Int. Ed. 42 (2003) 2782–2785.
[42] S. Ivanova, B. Louis, M.J. Ledoux, C. Pham-Huu, J. Am. Chem. Soc. 129 (2007) 3383–3391.